PHYSICAL REVIEW E **79**, 065302(R) (2009)

Three-dimensional poor man's Navier-Stokes equation: A discrete dynamical system exhibiting $k^{-5/3}$ inertial subrange energy scaling

J. M. McDonough*

Departments of Mechanical Engineering and Mathematics, University of Kentucky, Lexington, Kentucky 40506-0503, USA

(Received 8 September 2008; revised manuscript received 2 April 2009; published 3 June 2009)

Outline of the derivation and mathematical and physical interpretations are presented for a discrete dynamical system known as the "poor man's Navier-Stokes equation." Numerical studies demonstrate that velocity fields produced by this dynamical system are similar to those seen in laboratory experiments and in detailed simulations, and they lead to scaling for the turbulence kinetic energy spectrum in accord with Kolmogorov K41 theory.

DOI: 10.1103/PhysRevE.79.065302 PACS number(s): 47.27.−i

The "poor man's Navier-Stokes (PMNS) equation" (epithet taken from Frisch [1] where it is applied to a simple quadratic map) is a discrete dynamical system (DDS)—hence, very inexpensively evaluated (implying appropriateness of term "poor man's")—derived directly from the incompressible Navier-Stokes (N-S) equations. It provides a local (in space) model that is related to a pseudodifferential operator of these equations; thus we expect the PMNS equation to be capable of producing local time series at least in qualitative agreement with laboratory measurements and/or direct numerical simulation (DNS). Hence, it should be a useful contribution to high-fidelity subgrid-scale (SGS) models for large-eddy simulation (LES), leading to an ability to simulate interactions of turbulence with other physical phenomena in the inertial subrange scales and possibly below.

A thorough description of the DDS properties for what might be associated with isotropic turbulence is provided by McDonough and Huang [2], and this work was extended to further examination of effects of various combinations of bifurcation parameters (including anisotropic cases) by McDonough *et al.* [3] and sensitivity to initial conditions (SIC) by Bible and McDonough [4]. Yang *et al.* [5] have shown that the two-dimensional (2D) PMNS equation can be fit to local laser-doppler anemometry (also called velocimetry) measurements of flow over a backward-facing step, and McDonough and Zhang [6] further extended the work of [2] to treatment of chemical reactions, and in particular demonstrated good qualitative agreement with nonpremixed H_2-O_2 turbulent jet combustion measurements.

All of the above cited references report studies in two (physical) space dimensions. Here, we present a few of the salient features of the three-dimensional (3D) PMNS equation in the absence of any further physics. In what follows we first briefly outline the derivation of this DDS and note some of its analytical properties. We then show example time series and (frequency) power spectra for a turbulent state corresponding to 3D homogeneous, isotropic turbulence. Following this, we present what may be the most important result arising from the PMNS equation, at least in the context of its possible use in LES turbulence models—namely, $k^{-5/3}$ energy decay in the inertial subrange. We remark that results presented here are not intended to be all inclusive; a far more comprehensive treatment is in progress.

The starting point for deriving the PMNS equation is the incompressible N-S equation, sans the pressure gradient term (hence, related to a Leray projected form):

$$\boldsymbol{U}_t + \boldsymbol{U}\cdot\boldsymbol{\nabla}\boldsymbol{U} = \frac{1}{\mathrm{Re}}\Delta\boldsymbol{U} \quad \text{on} \quad \Omega\times(t_0,t_f]. \tag{1}$$

The subscript t denotes partial differentiation with respect to time; $\boldsymbol{\nabla}$ and Δ are gradient and Laplace operators, respectively (here, in Cartesian coordinates). Re is the Reynolds number: $\mathrm{Re}=UL/\nu$ with U and L being velocity and length scales, and ν the usual kinematic viscosity. $\boldsymbol{U}\equiv(u,v,w)^T$ is the velocity vector. Finally, Ω is a bounded domain in $\mathbb{R}^3$ with at least Lipschitz boundaries.

The next step is to assume components of $\boldsymbol{U}$ can be represented as Fourier series (see, e.g., Foias *et al.* [7] for justification),

$$\begin{pmatrix} u \\ v \\ w \end{pmatrix}(\boldsymbol{x},t) = \sum_{\boldsymbol{k}=-\infty}^{\infty} \begin{pmatrix} a_{\boldsymbol{k}} \\ b_{\boldsymbol{k}} \\ c_{\boldsymbol{k}} \end{pmatrix}(t)\varphi_{\boldsymbol{k}}(\boldsymbol{x}), \tag{2}$$

with $\{\varphi_{\boldsymbol{k}}\}$ being a complete (in L^2, a Hilbert space corresponding to finite energy) orthonormal basis exhibiting complex exponential-like properties with respect to differentiation, and $\boldsymbol{x}\in\mathbb{R}^3$. Substitution of Eq. (2) into Eq. (1) and carrying out the usual Galerkin procedure results in a (countably) infinite system of ordinary differential equations (ODEs) for the Fourier coefficients of the form (e.g., for the x-momentum equation)

$$\dot{a}_{\boldsymbol{k}} + A^{(1)}_{\boldsymbol{k}\ell\boldsymbol{m}}a_\ell a_{\boldsymbol{m}} + B^{(1)}_{\boldsymbol{k}\ell\boldsymbol{m}}a_\ell b_{\boldsymbol{m}} + C^{(1)}_{\boldsymbol{k}\ell\boldsymbol{m}}a_\ell c_{\boldsymbol{m}} = -\frac{|\boldsymbol{k}|^2}{\mathrm{Re}}a_{\boldsymbol{k}},$$

$$k_i = 0,1,\ldots,\infty, \quad i=1,2,3, \tag{3}$$

where the $A^{(1)}_{\boldsymbol{k}\ell\boldsymbol{m}}$, $B^{(1)}_{\boldsymbol{k}\ell\boldsymbol{m}}$, and $C^{(1)}_{\boldsymbol{k}\ell\boldsymbol{m}}$ are Galerkin triple products (but including wave number factors for convenient notation); e.g., $A^{(1)}_{\boldsymbol{k}\ell\boldsymbol{m}}\equiv(\ell_1+m_1)\int\varphi_{\boldsymbol{k}}\varphi_\ell\varphi_{\boldsymbol{m}}$. The superscript (1) denotes the first (x-) momentum equation, and $\boldsymbol{k}\equiv(k_1,k_2,k_3)^T$ suggests the meaning of the subscripts; $|\boldsymbol{k}|$ is the usual vector magnitude which we will sometimes represent as k (without a subscript) in the sequel.

*jmmcd@uku.edu; http://www.engr.uky.edu/~acfd

We remark that the ODEs consisting of Eq. (3), along with the analogous equations for $b_{\boldsymbol{k}}$ and $c_{\boldsymbol{k}}$, comprise a DNS (albeit, not a very efficient one) of the N-S equations (modulo some means for guaranteeing satisfaction of $\boldsymbol{\nabla}\cdot\boldsymbol{U}=0$) if truncated at sufficiently high $\boldsymbol{k}$ that $|\boldsymbol{k}|^2/\mathrm{Re}$ is large enough to provide the dissipation needed to control effects of the nonlinear terms on the left-hand side of Eq. (3). In particular, it is possible to produce nontrivial velocity fields without explicit pressure gradient forcing; moreover, formal elimination of the pressure gradient within the Galerkin procedure leads to additional terms of the same form as those arising from the advection terms.

Our goal here is completely different from producing a DNS procedure: we wish to obtain a very efficiently evaluated dynamical system that might be employed as part of a SGS model in the context of LES. One approach would be to construct a shell model such as those discussed in Bohr *et al.* [8] and numerous references therein, but we have chosen a different method. Namely, we discard all wave vectors in Eq. (3) except a single arbitrary one. Note that this is similar to a technique used in deriving the Lorenz equations (see, e.g., Yorke and Yorke [9]), except in that case the retained wave vector is specified (the lowest one—which would not be of much use in SGS model construction for LES). We remark that extending the formulation presented below to include additional wave numbers (e.g., so as to satisfy triad constraints) would be straightforward, and we plan to consider this in future studies associated with SGS models. Indeed, this was done in 2D for the data-fitting analyses of Yang *et al.* [5], but it has not yet been carried out in 3D largely because the SGS models constructed using a single wave vector for each instance of the DDS have worked well, both in the sense of at least qualitative accuracy and with respect to good load balancing between resolved- and small-scale LES calculations.

Suppression of wave vector subscript notation in this single wave number case permits expressing Eq. (3) as

$$\dot{a} + A^{(1)}a^2 + B^{(1)}ab + C^{(1)}ac = -\frac{|\boldsymbol{k}|^2}{\mathrm{Re}}a. \tag{4}$$

We observe that Eq. (4), along with similar forms corresponding to the y- and z-momentum equations, is a continuous dynamical system of sufficient phase-space dimension to admit chaotic solutions.

The PMNS equation derivation is completed by first applying forward-Euler temporal discretization leading to

$$a^{(n+1)} = a^{(n)} - \tau\left[\frac{|\boldsymbol{k}|^2}{\mathrm{Re}}a^{(n)} + A^{(1)}a^{(n)2} + B^{(1)}a^{(n)}b^{(n)} + {}^{(1)}a^{(n)}c^{(n)}\right], \tag{5}$$

with analogous results for $b^{(n+1)}$ and $c^{(n+1)}$; here τ is the numerical time step size, and superscripts (n) denote time-step index or, more appropriately, a map iteration counter. We now apply two transformations to obtain a more convenient form. The first of these was introduced in Ref. [2] and serves to convert the quadratic map portion of Eq. (5) to a logistic map form by setting $\tau A^{(1)} = 1 - \tau|\boldsymbol{k}|^2/\mathrm{Re} \equiv \beta_1$. Observe that this reduces the number of bifurcation parameters by one in each of the three equations. It has been shown by Bible [10] that this also expands the range of bifurcation parameter values over which nondivergent trajectories can be generated by the DDS (a valuable property for modeling applications). The second transformation is the well-known logistic map scaling of May [11], $\beta_i \mapsto 4\beta_i$, $i=1,2,3$ in 3D. The final result is the 3D poor man's Navier-Stokes equation

$$a^{(n+1)} = \beta_1 a^{(n)}(1-a^{(n)}) - \gamma_{12}a^{(n)}b^{(n)} - \gamma_{13}a^{(n)}c^{(n)}, \tag{6a}$$

$$b^{(n+1)} = \beta_2 b^{(n)}(1-b^{(n)}) - \gamma_{21}a^{(n)}b^{(n)} - \gamma_{23}b^{(n)}c^{(n)}, \tag{6b}$$

$$c^{(n+1)} = \beta_3 c^{(n)}(1-c^{(n)}) - \gamma_{31}a^{(n)}c^{(n)} - \gamma_{32}b^{(n)}c^{(n)}. \tag{6c}$$

This DDS exhibits several features worth mentioning. First, it is three dimensional and contains nine bifurcation parameters (β_i, $i=1,2,3$ and the γ_{ij}s, $i,j=1,2,3$, $i\neq j$); hence, it is mathematically intractable from a pure analysis perspective. (Lyubich [12] has noted that 2D DDSs might well be considered the mathematics "problem of the 21st century.") Hence, all results to be reported herein have been obtained via numerical computation. Second, (the arbitrary) wave number components and numerical time step size have been embedded in the bifurcation parameter definitions. Next, DDS (6) possesses a "structural symmetry" analogous to that of the N-S equations, themselves, and which is not found in most other dynamical system models; viz., all three equations take identical forms. In this regard, it is clear that if the bifurcation parameters are set so that $\beta_1=\beta_2=\beta_3$ and all γ_{ij}s are equal, one might expect to obtain the same time series for all of a, b and c, modulo effects from SIC. (The corresponding 2D case was analyzed exhaustively in Ref. [2] and constitutes a rather extreme form of isotropy.) Moreover, this symmetry is lacking in the Lorenz equations and in most shell models, e.g., that of Beck [13] in which the logistic map (not transformed as in Ref. [11]) is used as forcing for an otherwise linear model including some random coefficients.

Finally, we observe that the nature of the construction of Eq. (6), disregarding the final transformations, is analogous to deriving a pseudodifferential operator of a partial differential equation (PDE) (in this case, the N-S equations) which is carried out by first Fourier transforming the PDE, and then inverse transforming the result, producing (after some manipulations) an integral form of the PDE (hence, a pseudodifferential operator—see Treves [14]). Within this context consideration of only a single wave vector, as in the present case, corresponds to a form of microlocal analysis often employed in the study of pseudodifferential operators. Furthermore, by considering only a single wave vector we obtain a trivial form of Eq. (2), which would correspond to the inversion needed to complete pseudodifferential operator construction in the present countably infinite basis case. In particular, use of the Fourier series representations is the analog of Fourier inversion in the more usual application of Fourier transforms in a pseudodifferential operator context.

In the present brief work we will focus on only one point of a bifurcation diagram analogous to those provided in Refs. [2–4], corresponding to chaotic behavior of the PMNS equation solutions. All β_i values are 3.9, and all γ_{ij}s have a value

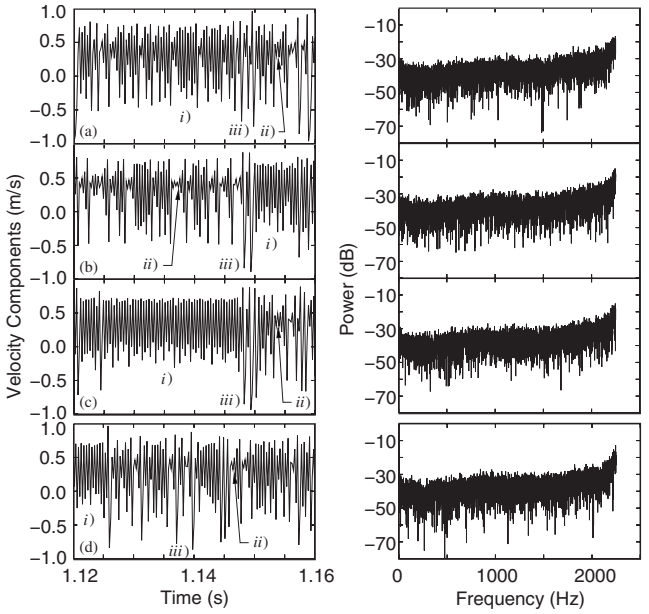

FIG. 1. Velocity components, with indication of "structure" type, and corresponding power spectra; (a) u component, (b) v component, (c) w component, and (d) u component with different initial conditions.

0.2. Equation (6) is evaluated for 10^4 iterations using 64-bit arithmetic, starting with initial conditions $a^{(0)}=e/10$, $b^{(0)}=\sqrt{2}/2$, and $c^{(0)}=\sqrt{3}/3$ [except for part (d) of Fig. 1—see below]. The last 9000 of these data points are employed in statistical analyses other than calculation of power spectral densities (PSDs) for which 8192 points were employed. With assumed length and velocity scales of unity, the Reynolds number is simply $\mathrm{Re}=1/\nu$; we take ν to be that for air at standard conditions.

Time series are run to obtain a 2 s interval of data for statistical analysis. Figure 1 displays only a very small subinterval (somewhat arbitrarily chosen near the center of the overall interval) to permit clear presentation of the detailed structure of the fluctuations. We observe that the raw output from the PMNS equation generally lies in the interval $[0,1+\mu]$ with $\mu<0.4$, typically (but depending in detail on combinations of bifurcation parameter values and, hence, on the associated trajectories) for nondivergent behaviors. This is generally inconvenient for modeling purposes, and we usually shift the observed interval to $[-1,1]$. In the present case we have done this in a manner that preserves the original relative amplitudes among the three components.

We first note that the power spectra for all three velocity components, shown in the right-hand sides of parts (a)–(c) of Fig. 1, are essentially identical, up to locations of "dropouts;" they all correspond to broad-band behavior, but with a remnant of the fundamental frequency still persisting. Moreover, although instant-to-instant details of the three velocity component time series shown on the left sides of these figures are quite different, it is clear that these all contain the same types of "structures;" one can observe (at least) the following three main types: (i) relatively long intervals of nearly periodic (actually subharmonic) behavior (hence, persistence of the fundamental frequency seen in the PSDs) with moderate amplitude peak-to-peak oscillations, (ii) generally much shorter periods of very low peak-to-peak amplitude fluctuations, and (iii) quite short-duration high-amplitude bursts. But these structures appear with varying numbers and lengths (in time) of occurrence for each of the three velocity components in the short interval displayed here and, in fact, for the complete time series (not shown). This stationarity of velocity component time series over long intervals implies energy conservation in the sense of L^2 and suggests that nonlinear advective and linear diffusive (dissipative) terms of Eqs. (3) and (4) are in balance for the chosen set of bifurcation parameters.

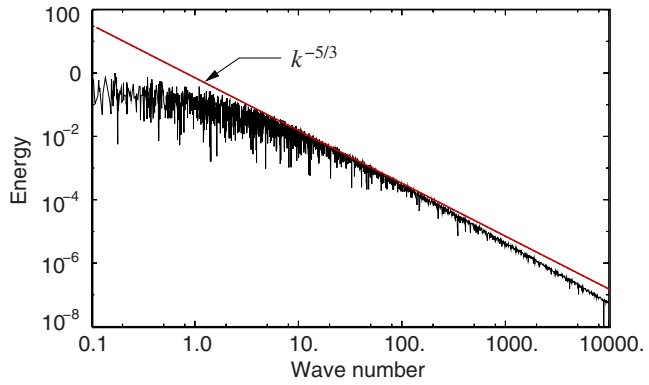

FIG. 2. (Color online) Turbulence kinetic energy vs wave number.

Finally, part (d) of Fig. 1 presents data for only the first component of velocity, obtained from a separate calculation in which all components of the initial data have been increased by 0.0001, and intended to demonstrate the SIC property of the PMNS time series for the bifurcation parameter values under consideration here. It is clear from the figure that the power spectrum has remained essentially unchanged, as is true for various statistics of the time series (to be treated in more detail in a forthcoming work). The left-hand side of part (d) presents the time series for the u component of PMNS velocity and should be compared with part (a) of the figure. We can identify the same types of structures, but their sequencing is seen to be different, as would be expected in comparisons of separate turbulent-flow experimental runs made under the same nominal conditions. It is clear by comparing these two figures that the time series displayed in part (d) cannot be produced by a mere phase shift of that in part (a); hence, the SIC property observed in turbulent flow experiments is also exhibited by PMNS equation time series. But in addition it appears likely that topology of underlying attractors must be very similar, as must almost always be the case in laboratory investigations—modulo slight variations in physical bifurcation parameters near fractal regime boundaries.

In Fig. 2 we demonstrate success of the PMNS equation in reproducing the Kolmogorov $k^{-5/3}$ energy decay in the inertial subrange. This is a relatively easy calculation since the dispersion relation for the formula associated with Taylor's hypothesis leads directly to conversion from (temporal) frequency, ω, to (spatial) wave number, k. Figure 2 displays results obtained in this way. It exhibits an integral scale of

low wave numbers, approximately a decade of inertial subrange, and then the beginnings of dissipation scales. The somewhat limited extent of the inertial subrange is not inconsistent with the moderate value of Re being considered ($\sim 7 \times 10^4$, based on physical scales mentioned earlier). We also remark that structure function scaling exponents, including those at second order, (to be presented in work in progress) do not perfectly agree with K41 theory but rather behave as observed in physical experiments—evidently exhibiting intermittency effects.

Finally, we observe that the power of the energy spectrum beyond a wave number of less than approximately 1000 decays with an exponent of -2, consistent with the beginning of dissipation; however, this does not change even at extremely high wave numbers (beyond those displayed in Fig. 2), implying that the PMNS equation alone cannot adequately represent the dissipation scales (at least when run with the current set of bifurcation parameters and/or single wave vector) or, correspondingly, alone does not supply sufficient numerical dissipation to control aliasing in underresolved LES.

The results reported in this work show a strong correlation of behavior, in terms of time series and energy vs wave number spectrum, of the poor man's Navier-Stokes equation and the full PDE Navier-Stokes equations. We submit that this is not accidental; the PMNS equation has been derived from the N-S system and is related to a pseudodifferential operator of these equations. As a consequence, one should expect that local behavior would show good agreement with that of the N-S equations, leading to the conclusion that the PMNS equation might provide a suitable starting point for various easily evaluated algebraic models of N-S system behavior on subgrid scales, as needed in LES formulations requiring a more detailed account of interactions of turbulence with other physical phenomena than can be expected from the usual filtered-equation/modeled-SGS-stress formalisms.

[1] U. Frisch, *Turbulence* (Cambridge University Press, Cambridge, England, 1995).
[2] J. M. McDonough and M. T. Huang, Int. J. Numer. Methods Fluids **44**, 545 (2004).
[3] J. M. McDonough, S. A. Bible, and J. Scoville, J. Turbul. **4**, 1 (2003).
[4] S. A. Bible and J. M. McDonough, Int. J. Bifurcat. Chaos **14**, 2381 (2004).
[5] T. Yang, J. M. McDonough, and J. D. Jacob, AIAA J. **41**, 1690 (2003).
[6] J. M. McDonough and Sha Zhang, AIAA 32nd Fluid Dynamics Conference and Exhibit, St. Louis, 2002. Paper No. 2002–3172 (unpublished).
[7] C. Foias, O. Manley, R. Rosa, and R. Temam, *Navier-Stokes Equations and Turbulence* (Cambridge University Press, Cambridge, 2001).
[8] T. Bohr, M. H. Jensen, G. Paladin, and A. Vulpiani, *Dynamical Systems Approach to Turbulence* (Cambridge University Press, Cambridge, 1998).
[9] J. A. Yorke and E. D. Yorke, in *Hydrodynamic Instabilities and the Transition to Turbulence*, edited by H. L. Swinney and J. P. Gollub (Springer-Verlag, Berlin, 1981).
[10] S. A. Bible, MS thesis, University of Kentucky, 2004.
[11] R. M. May, Nature (London) **261**, 459 (1976).
[12] M. Lyubich, Not. Am. Math. Soc. **47**, 1042 (2000).
[13] C. Beck, Phys. Rev. E **49**, 3641 (1994).
[14] F. Treves, *Introduction to Pseudodifferential and Fourier Integral Operators, Vol. 1 Pseudodifferential Operators* (Plenum Press, New York, 1980).